Nuclear Instruments and Methods in Physics Research B 345 (2015) 69–73

Contents lists available at ScienceDirect

Nuclear Instruments and Methods in Physics Research B

journal homepage: www.elsevier.com/locate/nimb

Radiance line ratios Ly-β/Ly-α, Ly-γ/Ly-α, Ly-δ/Ly-α, and Ly-ε/Ly-α for soft X-ray emissions following charge exchange between C^{6+} and Kr

V.M. Andrianarijaona [a,*], D. Wulf [b], D. McCammon [b], D.G. Seely [c], C.C. Havener [d]

[a] Department of Physics, Pacific Union College, Angwin, CA 94508, USA
[b] Department of Physics, University of Wisconsin, Madison, WI 53706, USA
[c] Department of Physics, Albion College, Albion, MI 49224, USA
[d] Physics Division, Oak Ridge National Laboratory, Oak Ridge, TN 37831-6372, USA

ARTICLE INFO

Article history:
Received 11 December 2014
Received in revised form 25 December 2014
Accepted 5 January 2015

Keywords:
Ion-atom collision
Charge transfer
Soft X-ray
Solar wind
Comet dusts

ABSTRACT

The radiance line ratios Ly-β/Ly-α, Ly-γ/Ly-α, Ly-δ/Ly-α, and Ly-ε/Ly-α for soft X-ray emission following charge exchange (CX) between C^{6+} and Kr are reported for collision energies between approximately 320 and 46,000 eV/u. The corresponding collision velocities (250–3000 km/s) are characteristic of the solar wind. X-ray spectra were obtained at the Oak Ridge National Laboratory Multicharged Ion Research Facility using a microcalorimeter X-ray detector with a resolution on the order of 10 eV FWHM. The measured Ly-ε/Ly-α is zero for all considered energies and suggests that very little, if any, capture to 6p occurs. The measured Ly-β/Ly-α and Ly-γ/Ly-α ratios intersect and form a well resolved node around (950 ± 50) km/s, which could be used as an astrophysical velocity indicative tool. The results reported here are compared to calculations for C^{6+} + H since no published theory for C^{6+} + Kr is known to exist. Double-electron-capture (DEC) and other multi-electron processes are possible. True double capture is estimated to be only 10% of the single-electron-capture (SEC).

1. Introduction

There is renewed interest in knowing the exact spectra of charge transfer (CX) induced soft X-ray emission. CX is critical to the understanding of the measured X-ray spectra from the ROSAT all-sky survey project (see for instance [1,2]), and consequently, laboratory measurements are highly desirable to enable the interpretation of these spectra [3,4]. The solar wind contains highly charged ions that capture electrons from the heliosphere neutral atoms and molecules into excited states which subsequently radiatively decay to lower states. In the case of a fully stripped ion such as C^{6+} or O^{8+}, the decay following CX involves a cascade of de-excitations filling inner shells, which leads to soft X-ray emission.

CX in collisions between fully-stripped ions and hydrogen atoms is of special interest because these systems have only one electron and thus single electron capture (SEC) is the only electron capture channel available. While the results of experimental investigations of such systems would provide very stringent tests of theoretical models, experiments are very challenging because of the difficulty to create H in the laboratory in sufficiently large number densities. While measurements of CX with H target are proposed using the ion-atom merged-beams apparatus at ORNL, gas cell measurements with other gas-phase targets have already been performed.

Previously, our measurements of C^{6+} + He, reported by Defay et al. [5], were compared with predictions by the Atomic-Orbital Close-Coupling (AOCC) calculations of Fritsch and Lin [6] and Molecular-Orbital Close-Coupling (MOCC) calculations of Kimura and Olson [7]. The experimentally determined Ly-β/Ly-α ratio is in good agreement with the AOCC predictions at higher collision energies (velocities above 1500 km/s) while the MOCC predictions exhibit the trend of the measured ratios at low collision energies. The measured Ly-γ/Ly-α ratio is surprisingly in good agreement with the predictions of AOCC at all energies studied. By contrast, theoretical line ratios of Kharchenko used in astrophysical modeling [8], are in poor agreement with the experimental results.

No theoretical work is known to exist that predicts the (n,l) resolved CX between highly charged ions and Kr. For Kr, the first ionization energy (14.0 eV) is very close to the hydrogen's (13.6 eV) and the SEC during its CX may mimic CX with hydrogen. Moreover, it is worthy to investigate if Kr might be a very good surrogate for H because its second and higher ionization potentials, which are respectively 24.4 and 37.0 eV, should be sufficiently high to limit double electron captures (DEC) and other multi-electron processes. From comparing the CX absolute cross section for

* Corresponding author.

http://dx.doi.org/10.1016/j.nimb.2015.01.002
0168-583X/

C^{6+} + H and the one for C^{6+} + H_2 that were measured by Meyer et al. [9], Fogle et al. [10] recently concludes that double capture autoionization (DCAI), which most measurements cannot distinguish from SEC, might be a significant process in low energy CX with H_2, limiting the possibility of using H_2 as a proxy for H at high energies only.

On the other side, it was shown by Andrianarijaona et al. [11] that, for CX involving molecular ions, the vibrational and rotational modes of the molecule affect the SEC cross section at low energies—which effects are to be added to the DCAI contribution. Therefore, investigating Kr represents a second interest because it is a very good test case for multi-electron target without the complication of the vibrational levels.

The measured SEC line ratios as well as the DEC line ratios will be presented here. Because no theory could be found for the X-ray emission following C^{6+} + Kr charge exchange, the discussion is based on theoretical calculations on (C^{6+}, H) and therefore refers to the SEC only. For this system, the SEC can be depicted as $C^{6+} + Kr \rightarrow C^{5+}$ (n,l) + Kr^{+} and is followed by cascades of the hydrogen-like ion to lower states, all of which end up to filling the 1s by emitting soft X-rays according to C^{5+} (n,l) $\rightarrow$ C^{5+} (1s) + $h\nu$.

A considerable number of theoretical investigations on C^{6+} + H, which include the works of Green et al. [12], Fritsch [13], Fritsch and Lin [14], Kimura and Lin [15], and Olson and Schultz [16], were published in the late eighties and by the end of the 20th century, there were few compilations of theoretical data for n,l-resolved cross sections [17–19]. For $n \leqslant 4$, the agreement amongst the different calculations looks surprisingly good and most calculations predicted that the SEC predominantly populate $n = 4$. However, there was a major spread in the data for $n = 5$, especially below 5 keV/u. These recommended and compiled cross sections were re-examined over the past few years, in particular by Caillat et al. [20], Liu et al. [21], and, Suno and Kato [22], pointing to the need for more (n,l) resolved measurements.

2. Apparatus

The experiment was conducted at ORNL-MIRF with the same experimental setup used for C^{6+} + He by Defay et al. [5] and Fogle et al. [10]. Fully stripped ^{13}C is produced in the permanent magnet Electron Cyclotron Resonance (ECR) ion source [23], magnetically selected to form a beam of $^{13}C^{6+}$ and then accelerated or de-accelerated off the high voltage platform to produce collisions with Kr at the solar wind velocities (300–2500 km/s).

As seen in Fig. 1, a microcalorimeter X-ray detector from a University of Wisconsin and Goddard Space Flight Center sounding rocket experiment, which was thoroughly described by McCammon et al. [24], is placed 23 cm above the beam line and, through a 2 cm opening, views a section of the beam line where CX take place with a Kr gas target at a constant pressure (3×10^{-4} Torr).

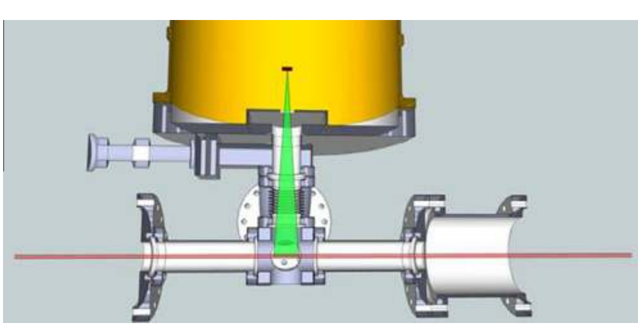

Fig. 1. Schemtaic of the microcalorimeter view of the C^{6+} beam as it passes through a beamline with Kr gas.

The ion beam current was a maximum of 60 nA for velocities above 1000 km/s (10 kV or 60 keV acceleration potential). However, the transmission of the beam is affected by the beam divergence, which increases at lower energies and reduces the beam intensity through the apparatus. Between 400 and 1000 km/s (2–10 kV acceleration potential), the ion beam current in the target cell was limited to 40 nA. The beam intensity dropped down to 2 nA at 365 km/s (1.5 kV acceleration potential) and was the low energy limit of our measurements. A typical run lasts roughly an hour at the highest beam energy and 2 h at the lower energies. Due to the thermal recovery time of the detector between events, the pressure in the gas cell was adjusted so the X-ray count rate of the detector was a few Hz. The small backgrounds from the ion beam (Kr gas valve closed), from the krypton target (ion beam valve closed), and from the dark count (both ion beam and Kr gas valves closed) were regularly measured and shown to be insignificant.

The X-ray detector is a 1×1.2 cm^2 microcalorimeter detector array and contains 36 pixels (see [24] for more details). Its resolution is better than 10 eV FWHM at 400 eV. It resolves without ambiguity the different line emissions of Ly-series for C VI that are emitted perpendicularly from the ion beam axis and viewed by the detector with a small solid angle (2.3e−3 sr). Likewise in the previous measurements reported by Defay et al. [5], the X-ray emission has been assumed to be isotropic and possible angular dependence with respect to the beam axis has not been taken into account. This is a reasonable assumption given that the comparison addressed ratios and that the $n = 2$ shell, which leads to Ly-α radiation, is populated by cascades from higher levels [25]. Therefore, the line ratios that are reported and discussed here, which are normalized by the Ly-α intensities, are assumed not to be affected by the emission anisotropies. During our entire measurements, the microcalorimeter X-ray detector was protected from infrared radiation by a series of thin carbon filters that were periodically defrosted. The filter transmission is energy dependent and has been determined with different detection efficiencies for the different Ly-series. The measured intensities were corrected for the energy-dependent transmission efficiencies of the filters, which are 0.0654, 0.1250, 0.1536, 0.1669, and 0.1743 for Ly-α–Ly-ε, respectively.

3. Results and discussions

A typical measured spectrum, like the ones presented in Fig. 2, has at least three or four Gaussian-like major peaks. Analogous to

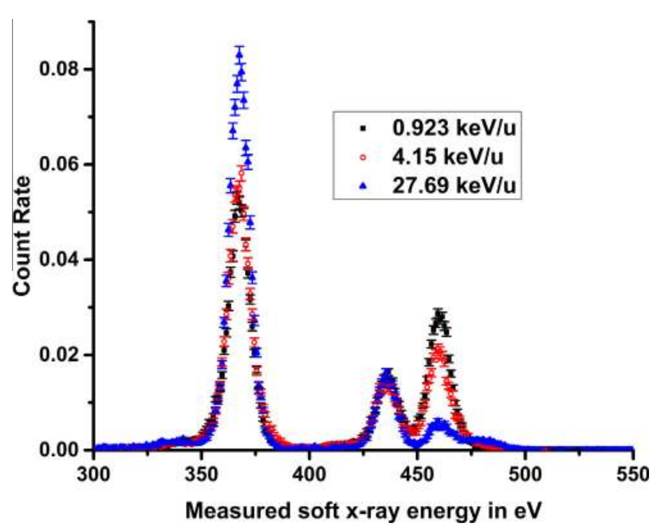

Fig. 2. Soft X-ray spectrum measured at 27.69, 4.15 and 0.923 keV/u corresponding to velocities of 2310, 895 and 517 km/s without any filter transmission correction.

previous measurements [5,10], the peaks have low-energy tails. They are thought to be due to pulse pileup in the detector since their size relative to the size of the central peak was observed to be directly correlated with the count rate. In order to identify each soft X-ray-related peak of the measured spectrum and to extract the area under it, the following Gaussian fit function was used

$$|A| + \sum_{i=1}^{13} |b_i| \frac{\exp\left(-4\ln(2)\frac{(x-a_i)^2}{v^2}\right)}{|v|\sqrt{\frac{4\pi}{\ln(2)}}}$$

where A is the background, a_i corresponds to the position of the Gaussian, b_i the area under it, and v the width. For most of the velocities, the software used (EasyPlot 4.0.5 from Spiral Software) could distinguish no more than 12 peaks, from which 10 seem to have averaged positions that could be directly compared to the C VI and C V line spectra from the National Institute of Standards and Technology (NIST) atomic spectra database found in http://www.nist.gov/pml/data/asd.cfm [26]. The ones that were identified as belonging to C VI lines, in another words emitted after a SEC, are listed in Table 1 and the others which are thought to be following a DEC are in Table 2. The pileup tails were subtracted using Gaussian fits, but with different widths. An example of the fit is presented in Fig. 3 with the corresponding measured spectrum.

The line ratios Ly-β/Ly-α, Ly-γ/Ly-α, Ly-δ/Ly-α, and Ly-ε/Ly-α, calculated by multiplying the ratio of Gaussian areas by the inverse ratio of filter efficiencies, are presented in Fig. 2. The variation of the Ly-β/Ly-α and Ly-γ/Ly-α with decreasing energy suggests that the SEC becomes more state-selective toward lower energies. The fact that the Ly-γ dominates toward lower energy, even though the Ly-β is still populated by cascades, suggests that the dominant SEC channel is to $n = 4$ and capture is strong in the p state. Ly-β/Ly-α and Ly-γ/Ly-α line ratios cross at about 950 km/s. If such a crossing exists for a particular system, the measured Ly-β/Ly-α ratio to the Ly-γ/Ly-α would be a convenient measure of the ion velocity. As seen in Figs. 4a and 4b, the Ly-ε/Ly-α is basically zero and the Ly-δ/Ly-α is flat and much smaller compared to the two other ratios, therefore SEC to the $n \geqslant 5$ levels may not go into small angular momentum states.

While there is no n,l specific published calculations for C^{6+} + Kr, since the first ionization potential of Kr is similar to H one can compare to calculations for C^{6+} + H. The predictions of Janev et al. [17] for (C^{6+}, H), which are based on the Atomic-Orbital Close-Coupling (AOCC) of Fritsch and Lin [14] and on a compilation of other varieties of data sources, agreed with the measurements of Hoekstra et al. [27] regarding the main capture states of the CT in C^{6+} + H, but calculate an increase in the capture to the $n = 5$p state. However, the measured Ly-δ/Ly-α C^{6+} + Kr indicate no significant capture to $n \geqslant 5$ at small l at low energy (see Figs. 4a and 4b).

Table 2
Identified DEC line spectra. The first column corresponds to the measured position (fit result) averaged on all energies. The STDV is in the second column. The third column contains the possible corresponding configuration. The fourth column was taken from NIST database for C V lines ($Z = 6$, He isoelectronic sequence) found in http://www.nist.gov/pml/data/asd.cfm [26]. The last value in the fourth column corresponds to the C VI (1s $^2S_{1/2}$) limit.

Averaged peak position (eV)	Standard deviation (eV)	Assigned configurations and transitions	NIST database (eV)
309.63	5.73	1s2p ($^3P^0_1$) to 1s^2 1s2p ($^1P^0_1$) to 1s^2	304.40069 307.89897
354.15	2.49	1s3p ($^3P^0_1$) to 1s^2 1s3p ($^1P^0_1$) to 1s^2	353.5293 354.51650
369.95	5.26	1s4p ($^3P^0_1$) to 1s^2 1s4p ($^1P^0_1$) to 1s^2	370.5093 370.91884
383.02	5.70	Unidentified	392.09049 (limit)

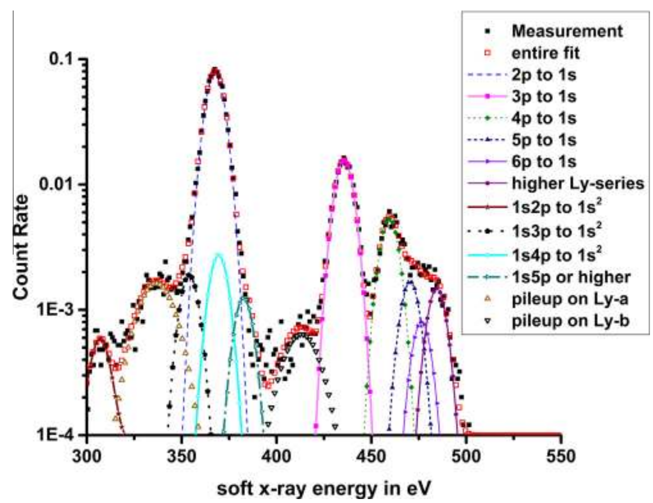

Fig. 3. Fit results for the spectrum measured at 27.69 keV/u in logarithmic scale.

Table 1
Identified SEC line spectra (Ly-series). The first column corresponds to the measured position (fit result) averaged on all energies. The STDV is in the second column. The third column contains the assigned line. The two values in the fourth column correspond to $J = 1/2$ (first line) and $J = 3/2$ (second line) from the NIST database (http://www.nist.gov/pml/data/asd.cfm) for C VI lines ($Z = 6$, H isoelectronic sequence) [26]. The limit of SEC emission is included in the last raw of the NIST database column.

Averaged peak position (eV)	Standard deviation (eV)	Assigned configurations and transitions	NIST database (eV)
367.52	0.16	2p (Ly-α) to 1s	367.4740214 367.5329097
436.34	0.35	3p (Ly-β) to 1s	435.54674516 435.56419411
459.62	0.37	4p (Ly-γ) to 1s	459.36980427 459.37716526
469.86	1.43	5p (Ly-δ) to 1s	470.39545519 470.39922385
477.65	3.03	6p (Ly-ε) to 1s	476.38427108 476.38645194
495.29	23.79	Unidentified 7p–1s 8p–1s 9p–1s	 *479.99583577* *482.33910217* *483.945601295* 489.993168 (limit)

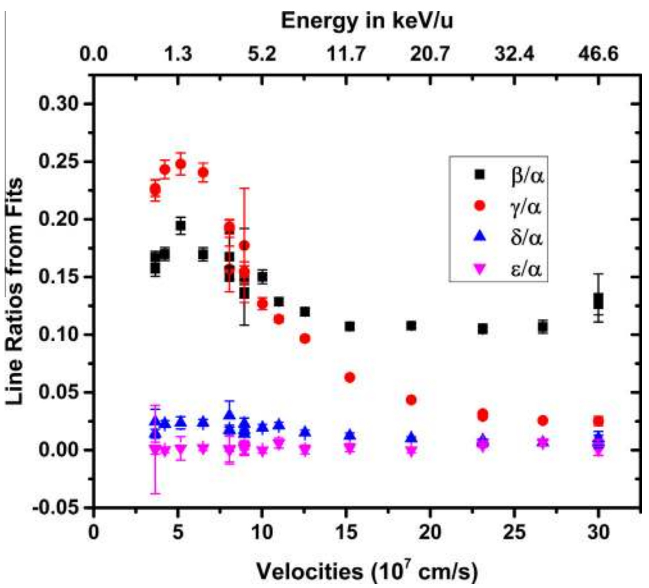

Fig. 4a. Line ratios from the fits. The area under the peaks (a_i in the fit function) were corrected by the transmission factor of the thin carbon foil shielding the microcalorimeter and by the coefficient of efficiency of the detector at the given line energy in order to get the line ratios. The error bars are 2σ and include both statistical uncertainty and systematic uncertainty arising from fits.

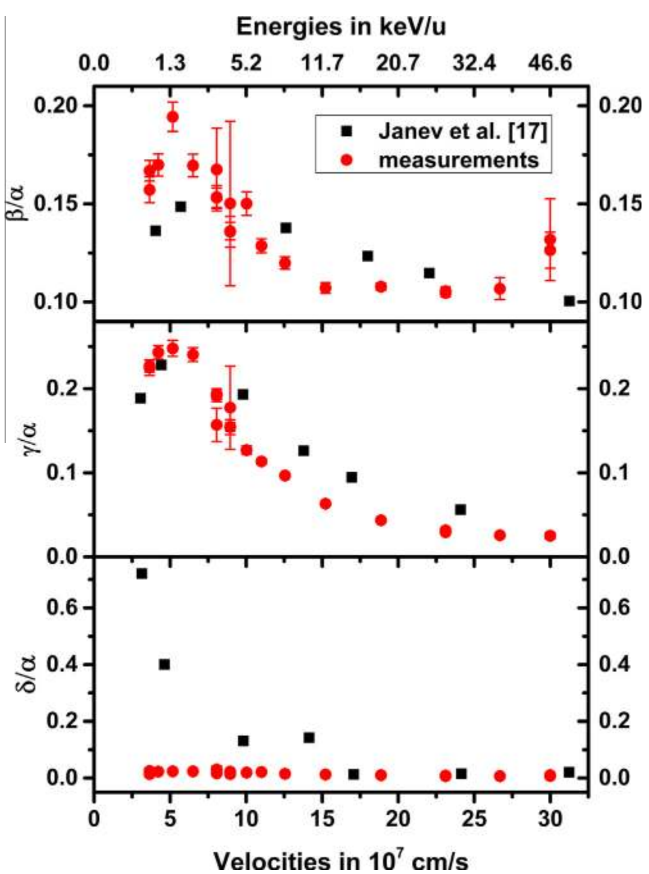

Fig. 4b. Measured Ly-δ/Ly-α line ratio of C^{6+} + Kr (see Fig. 4a) compared to the recommended data from [17] for C^{6+} + H (no theory on Kr could be found in the literatures).

Of course CX in (C^{6+}, Kr) collisions is more complicated than CX in (C^{6+}, H) because of the possibility of having multi-photon processes such as the double capture with auto-ionization (DCAI)

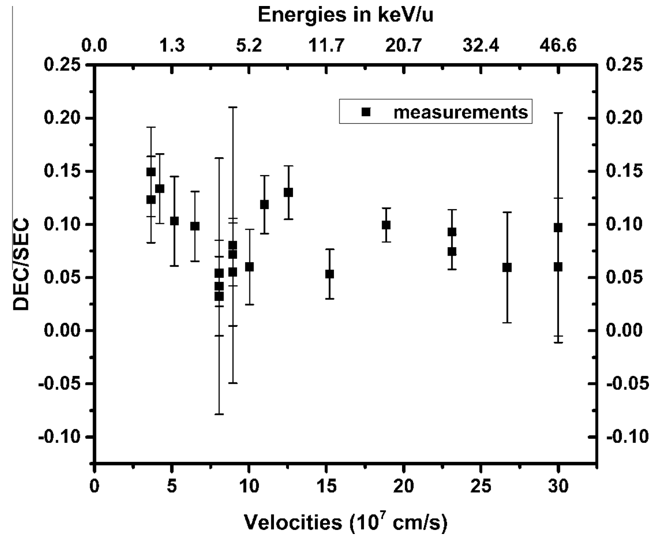

Fig. 5. Measured DEC/SEC. Summing all the areas corresponding to the identified peaks in Tables 1 and 2 after correcting them by the coefficient of efficiencies of the thin carbon shielding, the ratio DEC/SEC is obtained.

and transfer ionization (TI) during which one electron is capture and the other directly ionized. A preliminary comparison between the measured DEC and SEC is shown in Fig. 5. The ratio between all Ly-series emissions depicted in Table 2 (DEC) and a sum of all Ly-series emissions for SEC (Table 1) shows a relatively flat ratio and suggests that DEC takes between 5% and 15% of the charge transfer. Calculation for C^{6+} + Kr would be difficult because more channels are open. Different classical trajectory Monte Carlo (CTMC) models could be considered as it was already done for (C^{6+}, H_2) by Fogle et al. [10].

4. Conclusion

In conclusion, a crossing between the measured Ly-β/Ly-α and Ly-γ/Ly-α is observed around (950 ± 50) km/s and could be used as a velocity diagnostic tool in astrophysical observations. Our results provide a new set of recommended data on SEC and DEC charge exchange involving highly charged heavy ions or Kr, a multielectron target. Even though Kr and H have a similar first ionization potential, the recommended data for C^{6+} + H does not show the same low energy behavior.

Acknowledgments

This research is supported in part by the NASA Solar & Heliospheric Physics Program NNH07ZDA001N, NASA Grant No. NNX09AF09G, and by the Office of Fusion Energy Sciences and the Division of Chemical Sciences, Geosciences and Biosciences, Office of Basic Energy Sciences, U.S. Department of Energy. V.A. is supported by the National Science Foundation through Grant No. PHY-1068877.

References

[1] C.M. Lisse, K. Dennerl, J. Englhauser, M. Harden, F.E. Marshall, M.J. Mumma, R. Petre, J.P. Pye, M.J. Ricketts, J. Schmitt, J. Trümper, R.G. West, Science 274 (1996) 205.
[2] T.E. Cravens, Geophys. Res. Lett. 24 (1997) 105.
[3] K. Morgan, V.M. Andrianarijaona, I.N. Draganic, X. Defay, M. Fogle, A. Galindo-Uribarri, C.I. Guillen, C.C. Havener, M. Hokin, D. McCammon, D.J. Nader, S.L. Romano, F. Salces, F.S. Carcoba, P. Sauter, D. Seely, P.C. Stancil, C.R. Vane, A.K. Vassantachart, D. Wulf, AIP Conf. Proc. 1525 (2013) 49.
[4] J.K. Lepson, P. Beiersdorfer, E. Behar, S.M. Kahn, Nucl. Instr. Meth. B 235 (2005) 131.

[5] X. Defay, K. Morgan, D. McCammon, D. Wulf, V.M. Andrianarijaona, M. Fogle, D.G. Seely, I.N. Draganić, C.C. Havener, Phys. Rev. A 88 (2013) 052702.
[6] W. Fritsch, C.D. Lin, J. Phys. B 19 (1986) 2683.
[7] M. Kimura, R.E. Olson, J. Phys. B 17 (1984) L713.
[8] D. Koutroumpa, Doctoral thesis, Université Pierre et Marie Curie Verrières-le-Buisson, 2007.
[9] F.W. Meyer, A.M. Howald, C.C. Havener, R.A. Phaneuf, Phys. Rev. A 32 (1985) 3310.
[10] M. Fogle, D. Wulf, K. Morgan, D. McCammon, D.G. Seely, I.N. Draganić, C.C. Havener, Phys. Rev. A 89 (2014) 042705.
[11] V.M. Andrianarijaona, I.N. Draganić, D.G. Seely, C.C. Havener, Phys. Rev. A 84 (2011) 062716.
[12] T.A. Green, E.J. Shipsey, J.C. Browne, Phys. Rev. A 25 (1982) 1364.
[13] W. Fritsch, Phys. Rev. A 30 (1984) 3324.
[14] W. Fritsch, C.D. Lin, Phys. Rev. A 29 (1984) 3039.
[15] M. Kimura, C.D. Lin, Phys. Rev. A 32 (1985) 1357.
[16] R.E. Olson, D.R. Schultz, Phys. Scr. T28 (1989) 71.
[17] R.K. Janev, R.A. Phaneuf, H. Tawara, T. Shirai, At. Data Nucl. Data Tables 55 (1993) 201.
[18] N. Toshima, H. Tawara, NIFS Data 26 (1995) 1.
[19] C. Harel, H. Jouin, B. Pons, At. Data Nucl. Data Tables 68 (1998) 279.
[20] J. Caillat, A. Dubois, J.P. Hansen, J. Phys. B 33 (2000) L715.
[21] C.-N. Liu, S.-C. Cheng, A.-T. Lee, C.D. Lin, Phys. Rev. A 72 (2005) 012717.
[22] H. Suno, T. Kato, At. Data Nucl. Data Tables 92 (2006) 407.
[23] C.C. Havener, E. Galutschek, R. Rejoub, D.G. Seely, Nucl. Instr. Meth. B 261 (2007) 129.
[24] D. McCammon, K. Barger, D.E. Brandl, R.P. Brekosky, S.G. Crowder, J.D. Gygax, R.L. Kelley, C.A. Kilbourne, M.A. Lindeman, F.S. Porter, L.E. Rocks, A.E. Szymkowiak, J. Low Temp. Phys. 151 (2008) 715.
[25] J.B. Greenwood, I.D. Williams, S.J. Smith, A. Chutjian, Phys. Rev. A 63 (2001) 062707.
[26] NIST, Atomic spectra database. Found in <http://www.nist.gov/pml/data/asd.cfm>, 2014.
[27] R. Hoekstra, D. Ciric, F.J. de Heer, R. Morgenstern, Phys. Scr. T. 28 (1989) 81.